

A method for reversible drug delivery to internal tissues of *Drosophila* embryos

Victoria K Schulman,^{1,2} Eric S Folker¹ and Mary K Baylies^{1,2,*}

¹Program in Developmental Biology; Sloan Kettering Institute; Memorial Sloan-Kettering Cancer Center; New York, NY USA; ²Department of Cell and Developmental Biology; Weill Cornell Graduate School of Medical Sciences; Cornell University; New York, NY USA

Keywords: *Drosophila*, embryo, Chorion, permeabilization, drug delivery

Drosophila melanogaster is a powerful model organism to elucidate basic cellular mechanisms of development. Indeed, much of our understanding of genetic pathways comes from work in *Drosophila*. However, mutations in many critical genes cause early embryonic lethality; thus, it is difficult to study the role of proteins that are required for early fundamental processes during later embryonic stages. We have therefore developed a method to reversibly deliver drugs to internal tissues of stage 15–16 *Drosophila* embryos using a 1:1 combination of D-limonene and heptane (LH). Specifically, delivery of Nocodazole was shown to be effective as evidenced by the significant decrease in microtubule density seen in muscle cells. Following complete depolymerization of the microtubule cytoskeleton, removing the Nocodazole and washing for 10 min was sufficient for the microtubule network to be re-established, indicating that drug delivery is reversible. Additionally, the morphology of LH-treated embryos resembled that of untreated controls, and embryo viability post-treatment with LH was significantly increased compared with previously reported permeabilization techniques. These advances in embryo permeabilization provide a means to disrupt protein function in vivo with high temporal specificity, bypassing the complications associated with genetic disruptions as they relate to the study of late-stage developmental mechanisms.

Introduction

Drosophila melanogaster is a genetically tractable model organism that has been used to elucidate many basic tenets and pathways that control development. In the fly, mutational analyses have been critical for identifying novel factors required for various cellular and developmental processes. However, mutations in proteins that are fundamental to general cellular function often result in early embryonic lethality, making it difficult to study their roles in later stages of embryonic development. Temperature-sensitive alleles marginally alleviate this problem by permitting some temporal control of protein activity. However, the sensitivity of these alleles to temperature stress is ill-defined and there are many genes for which no such alleles exist. Tissue-specific depletion of proteins via RNA interference under the control of the temporally and spatially restricted GAL4/UAS system provides a more fine-tuned disruption of protein function, but this technique is not rapid or reversible and, for many genes, may not provide sufficient depletion of protein levels to cause a phenotype.^{1–3} Thus, the prime approaches to studying cell and developmental biology in *Drosophila* limit the study of many late-developing embryonic tissues. Therefore, to better understand biological mechanisms, we must develop a tool to more precisely manipulate protein function in vivo without permanently inhibiting cellular function.

Acute and reversible manipulation of cellular function is commonly achieved in tissue culture. Drugs can be delivered to cultured cells by simply bathing the cells in a solution containing the drug(s) of interest. These drugs can then be subsequently removed by exchanging the drug-containing media for media lacking the drug. Such approaches have been utilized to describe the physical organization of the mitotic spindle and the cell migration machinery among other basic cell biological processes.^{4,5} However, while there is much to be gained from these studies, cell culture systems cannot recapitulate 3-dimensional biological tissues, nor can they simulate the environment generated by neighboring tissues.

The primary hindrance to using drugs to disrupt protein function in *Drosophila* embryos has been the impermeability of the protective eggshell. The eggshell consists of 5 layers: the exochorion, the endochorion, the inner chorionic layer, the waxy layer, and the innermost vitelline membrane.⁶ The 3 outer chorionic layers can be easily removed with minimal adverse side effects by submerging embryos in 3% sodium hypochlorite (50% bleach). However, penetrating both the waxy layer and the vitelline membrane without affecting embryo viability is difficult. Microinjection techniques can deliver drugs through the vitelline membrane without deleterious effects on viability, but these methods are time-consuming, require individual manipulation of each embryo, only deliver the drug locally, and are irreversible.⁷

*Correspondence to: Mary K Baylies; Email: m-baylies@ski.mskcc.org
Submitted: 04/19/13; Revised: 06/14/13; Accepted: 06/17/13
<http://dx.doi.org/10.4161/fly.25438>

Even with automated injection of multiple embryos simultaneously, microinjection methods continue to be labor-intensive and insufficient for rapid screening, and they still lack reversibility.⁸

To overcome these challenges, a method of rendering the *Drosophila* embryo permeable to drug exchange is necessary. Such a technique must be optimized to meet several criteria. First, the procedure should prepare numerous embryos simultaneously to decrease workload and enable rapid screening of novel small molecule compounds *in vivo*. Second, the method must deliver drugs to internal tissues. The epithelial cell layer that covers the *Drosophila* embryo has a depth of 30 μm that must be traversed to reach endodermally- and mesodermally-derived tissues.⁹ Third, drug delivery must be reversible to facilitate study of the mechanisms associated with restoring and maintaining tissue integrity. Finally, to study late-developing tissues, permeabilization techniques must be applicable to older embryos without affecting viability, such that both tissue formation in the embryo and subsequent physiology at larval and/or adult stages can be assessed.

Existing embryo permeabilization protocols address some but not all of these criteria. Non-polar organic solvents, such as hexane, heptane, and octane have been used to permeabilize the vitelline membrane.^{10–13} However, treatment with these solvents decreased viability, particularly for young embryos.^{10,12,13} Alternatively, a combination of D-limonene with added surfactants, referred to as Embryo Permeabilization Solution (EPS), was used to permeabilize early embryos (up to stage 12, 0–8 h After Egg Laying, AEL) in the absence of alkanes.¹⁴ However, EPS only permitted the delivery of small molecules to the epidermis. Moreover, embryos between stages 9–12 (4–8 h AEL) treated with EPS were less viable than younger embryos treated with EPS.¹⁴ The minimal depth of penetration and the effects on embryo viability render this treatment ineffective for studying the development and function of internal tissues at later embryonic stages.

Therefore, we have developed a new protocol for delivering drugs to internal tissues of late-stage *Drosophila* embryos. A solution consisting of equal parts D-limonene and heptane (LH) effectively delivers drugs to the developing muscles of stage 15–16 embryos (13–16 h AEL) with improved viability over previously reported protocols. Furthermore, we can prepare embryos in batches, permitting both the analysis of large numbers of embryos simultaneously as well as rapid screening of novel compounds without the labor-intensive pitfalls of microinjection techniques. Finally, we demonstrate that we cannot only deliver drugs, but also remove these drugs. Altogether, our protocol combines important components of the previously documented techniques yet meets the necessary criteria for studying both tissue morphogenesis in late embryogenesis and behavioral function during larval and adult stages of development.^{12,14}

Results

Assay design. We aimed to develop a method of delivering drugs to internal tissues of late-stage *Drosophila* embryos to better elucidate cellular mechanisms of development *in vivo*. To develop this

protocol, we targeted the microtubule cytoskeleton and assessed the effects on microtubules in muscles. Muscle is a well-characterized, mesodermally-derived tissue that undergoes several distinct cellular and morphological changes late in embryogenesis. Thus, it is an ideal tissue in which to evaluate the delivery of drugs to older embryos. Microtubules are an ideal target for our assay as they are abundant, easily imaged, and a common pharmacological target. To specifically target microtubules, we used Nocodazole, an inhibitor of microtubule polymerization, to reduce the number of microtubules present. The effectiveness of drug delivery was then assessed by fluorescence imaging of both microtubules and growing microtubule plus-ends in fixed and live embryos, respectively.

Embryo handling

Functional myofibers are formed during late embryonic stages 14–17 (11–20 h AEL). As such, stage 15–16 embryos (13–16 h AEL) were collected using timed lays. Embryos were then submerged in 3% sodium hypochlorite (50% bleach) to remove the outer 3 chorionic layers, and subsequently washed with water for 5 min. Batches of embryos were then incubated with permeabilization solution supplemented with either 66 nM Nocodazole in dimethyl sulfoxide (DMSO) or DMSO alone and placed on a shaker to remove the waxy layer and penetrate the vitelline membrane. After removing the drug and rinsing in phosphate-buffered saline (PBS) to prevent desiccation, the embryos were examined in 1 of 3 ways. First, the total that survived to each developmental stage was quantified to assess viability post-treatment. Second, embryos from each treatment condition were used for fixed tissue analysis. Embryos fixed immediately following treatment (0 min after initial rinsing) were examined to determine if Nocodazole could be delivered to the embryo. Embryos that endured further washes in PBS for 2, 5, 10, or 30 min after manual drug removal prior to fixation were analyzed to determine if, and how quickly, Nocodazole could be removed from internal tissues of the embryo. All fixed embryos were immunostained with Tropomyosin and α -Tubulin antibodies to identify the muscles and determine whether microtubules were present in each of the different conditions. Immediately following drug treatment, the presence of microtubules indicated that Nocodazole was not effectively delivered to the muscles whereas the absence of microtubules indicated effective delivery of Nocodazole. Finally, a third set of embryos from each treatment condition were rinsed in PBS and mounted in halocarbon oil on a gas-permeable membrane for time-lapse analysis of ongoing microtubule polymerization (Fig. 1; refer to the Materials and Methods section for a more detailed description of procedures).

EPS is not sufficient to permeabilize late-stage embryos

An Embryo Permeabilization Solution (EPS) was recently reported that effectively permeabilized early *Drosophila* embryos.¹⁴ EPS consists of the monoterpene oil, D-limonene, which removes the waxy coat around the exterior of the vitelline membrane, and two surfactants, Biosoft® and Ninol®. EPS permeabilized early embryos up to stage 12 (0–8 h AEL), as evidenced by the uptake of dyes in the epidermis.¹⁴ However, the ability of EPS to permeabilize embryos beyond stage 12 of embryonic development was not assessed.

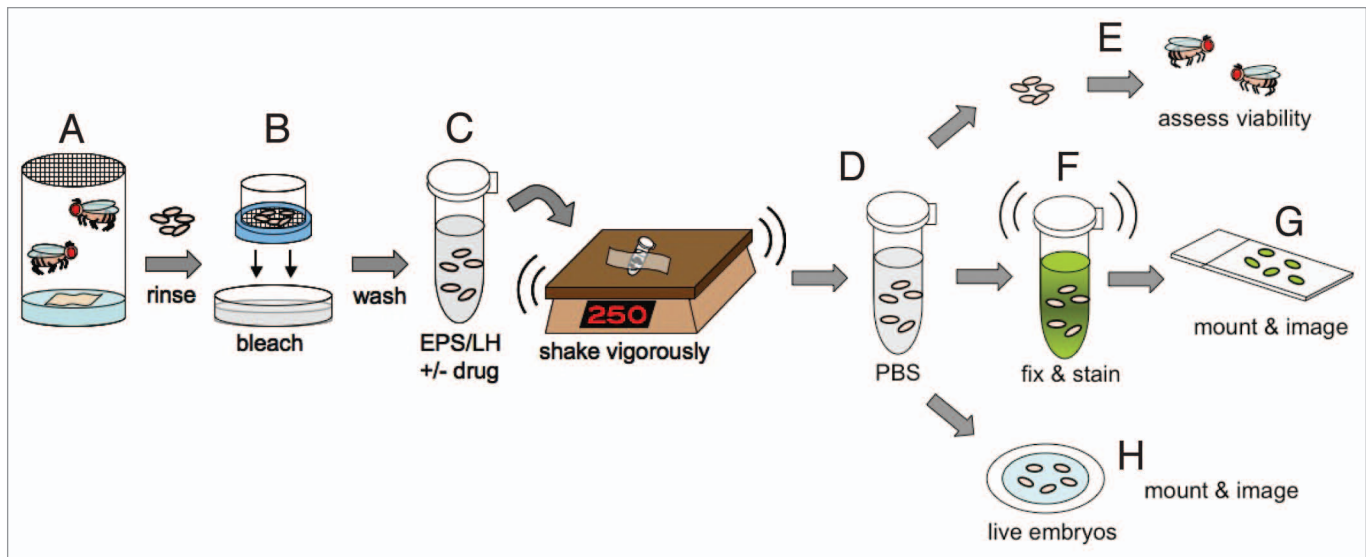


Figure 1. Embryo treatment procedures. (A) Embryos were harvested in laying pots containing adult flies of the appropriate genotype. (B) Embryos were dechorionated in 50% bleach for 4 min. (C) Embryos were then transferred to 1.7 ml eppendorf tubes containing permeabilization solution and drug or vehicle, adhered to a platform, and vigorously rotated at 250 rpm for defined lengths of time. (D) Post-treatment, embryos were rinsed in PBS before being analyzed in 1 of 3 ways (E–H). (E) After rinsing in PBS, embryos were assessed for viability. The total number that progressed to each stage of development was quantified. (F) Alternatively, embryos were further washed in PBS for defined durations prior to fixing the embryos and immunostaining for Tropomyosin and α -Tubulin. (G) Immunostained embryos were mounted on glass slides with coverslips and analyzed by confocal microscopy. (H) Alternatively, after rinsing with PBS, live embryos were prepared for time-lapse confocal microscopy.

To deliver Nocodazole to stage 15–16 embryos (13–16 h AEL), we used a 1:5::EPS:PBS solution for 5 min, conditions previously reported to deliver small molecules to *Drosophila* embryos.¹⁴ This solution was supplemented with either 66 nM Nocodazole in DMSO or DMSO vehicle control for our experiments. As a first measure of efficient delivery of Nocodazole to the muscles, we assessed viability post-treatment. After applying and removing Nocodazole, only 25% of embryos treated with 1:5::EPS:PBS for 5 min developed to adulthood compared with 48% of DMSO vehicle controls ($n \geq 300$; Fig. 2A). Furthermore, a 5 min treatment achieved maximal effects on viability, as 20 and 60 min treatments produced similar results. The decline in viability suggested that 1:5::EPS:PBS might be capable of delivering drugs to internal tissues of the embryo.

To determine whether Nocodazole was successfully delivered to the muscle cells in embryos treated with 1:5::EPS:PBS, the embryos were fixed and immunostained for α -Tubulin and Tropomyosin, and the presence/absence of microtubules in the muscle cells was assessed. There was no difference in microtubule density between drug treatments or vehicle controls, indicating that a 5 min treatment of embryos with Nocodazole in 1:5::EPS:PBS is not sufficient to deliver Nocodazole to the musculature of stage 15–16 embryos ($n \geq 300$; Fig. 2B–D, and G).

The *Drosophila* eggshell becomes sturdier over time.^{15–17} Consistent with this notion, embryos between stages 9–11 (4–6 h AEL) required longer treatments with 1:5::EPS:PBS than embryos between stages 4–8 (2–4 h AEL) to achieve comparable degrees of permeabilization.¹⁴ However, increasing the duration of drug treatments in 1:5::EPS:PBS for stage 15–16 embryos (13–16 h AEL) up to 60 min did not affect the microtubule

network in the muscles ($n \geq 300$; Fig. 2C, and E–G). Together, these data indicate that the previously described EPS solution is not an effective means by which to deliver drugs to the muscles of late-stage embryos.

EPS disrupts normal development and compromises viability

Ideally, the means of drug delivery itself would be benign to embryonic development. However, 1:5::EPS:PBS treatment on its own reduces viability to 48% compared with 82% for untreated counterparts, suggesting that EPS disrupts normal development (Fig. 2A). Furthermore, 21% of the embryos treated with 1:5::EPS:PBS alone displayed disruptions of the stereotypic pattern of repeated hemisegments seen in the musculature of *Drosophila* embryos ($n \geq 300$; Fig. 2H, compare with Fig. 2B). These data suggest that EPS itself causes deleterious effects on overall tissue organization. Finally, the larvae that hatched post-treatment with 1:5::EPS:PBS were all significantly smaller (Fig. 2I) and exhibited reduced motility compared with controls by gross examination. Together, these data suggest that EPS-mediated drug delivery is limited by both its poor ability to deliver drugs to internal tissues and its dramatic effects on organismal development.

D-limonene is not detrimental to developing embryos but is insufficient for embryo permeabilization

We deconstructed the EPS solution to determine whether D-limonene or the surfactants caused the observed developmental defects. We treated embryos with D-limonene alone and found that 74% of treated embryos survived to adulthood compared with 82% of untreated controls ($n \geq 300$; Fig. 3A). Additionally, larvae that hatched from embryos treated with D-limonene alone resembled controls in both size and gross

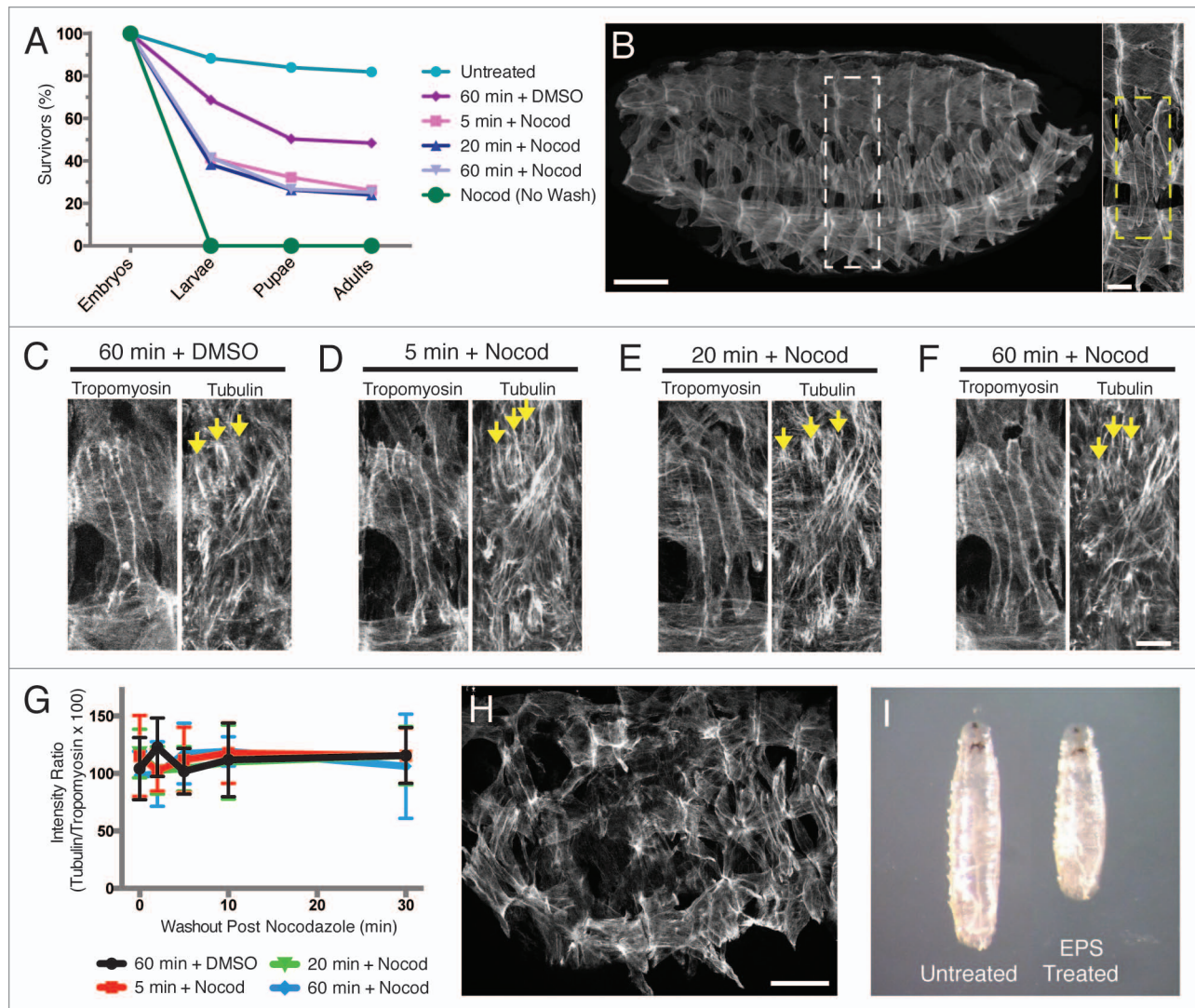


Figure 2. EPS is not sufficient to permeabilize late-stage embryos and is detrimental to normal *Drosophila* development. **(A)** Graph of viability of 1:5::EPS:PBS-treated embryos following washout of either drug or vehicle control (unless otherwise noted). **(B, left)** Wild-type stage 16 (16 h AEL) *Drosophila* embryo oriented with anterior to the left and dorsal up, immunostained for Tropomyosin to show muscles. Scale bar, 50 μ m. **(Right)** Higher magnification of white dashed box outlining 1 hemisegment. Yellow dashed box highlights the 4 Lateral Transverse (LT) muscles within a hemisegment. Scale bar, 10 μ m. **(C–F)** Stage 16 embryos treated for the indicated length of time with 1:5::EPS:PBS and either DMSO vehicle control or 66 nM Nocodazole in DMSO, removed from drug/EPS solution without further washout, immediately fixed, and immunostained with α -Tubulin and Tropomyosin antibodies to label the microtubules and the muscle cells, respectively. Arrows indicate selected microtubules near the dorsal poles of the LT muscles. Scale bar, 10 μ m. **(C)** Sixty minute treatment with 1:5::EPS:PBS and DMSO vehicle control. **(D)** Five minute treatment with 1:5::EPS:PBS and 66 nM Nocodazole in DMSO. **(E)** Twenty minute treatment with 1:5::EPS:PBS and 66 nM Nocodazole in DMSO. **(F)** Sixty minute treatment with 1:5::EPS:PBS and 66 nM Nocodazole in DMSO. **(G)** Quantification of immunofluorescence intensity of α -Tubulin detected in each treatment condition shown in **(C–F)** over time after the removal of Nocodazole (Note: all 4 data sets fall on top of one another). **(H)** Stage 16 embryo treated with DMSO vehicle control in 1:5::EPS:PBS for 20 min immunostained for Tropomyosin (compare with **[B]**). Scale bar, 50 μ m. **(I)** Comparison of larval size in L3 wandering larvae.

motility (data not shown). The improvements in viability and larval health indicate that D-limonene does not perturb development.

We next tested whether D-limonene was sufficient to deliver drugs to the embryonic musculature. Treatment with 66 nM Nocodazole in D-limonene for up to 20 min did not affect the microtubules in the muscle cells ($n \geq 300$; **Fig. 3D and F**). These data indicate that D-limonene is not sufficient to deliver drugs to the muscles of late-stage *Drosophila* embryos.

A combination of D-limonene and heptane maintains significant embryo viability post-treatment

We next explored additional D-limonene-based chemical combinations as a means to deliver drugs to *Drosophila* embryos, focusing on the addition of alkanes because they are known to permeabilize the vitelline membrane.^{10–13,18} Heptane was examined because it is less deleterious than other alkanes in embryos stage 12 and older (> 8 h AEL).¹² Of note, while heptane effectively permeabilizes embryos, treatment with heptane alone resulted in embryonic lethality (100%, $n \geq 300$).

Interestingly, many heptane-treated embryos exhibited extreme desiccation, which was not observed with D-limonene alone, despite that both heptane and D-limonene are organic solvents. Hypothesizing that heptane could provide the desired permeability while D-limonene could simultaneously prevent dehydration and enhance permeability, we tested whether a combination of the 2 solvents could deliver drugs to the musculature without perturbing development.

We found that 72% of embryos treated with a solution consisting of equal parts D-limonene and heptane (hereafter referred to as LH) survived to adulthood compared with 82% of untreated embryos ($n \geq 300$; Fig. 3A). Importantly, viability of LH-treated embryos was similar to D-limonene-treated embryos (74%), but much greater than both heptane-treated embryos (0%) and 1:5::EPS:PBS-treated embryos (48%). Furthermore, 100% of LH-treated embryos displayed the stereotypic organization of hemisegments in the muscle pattern as seen in untreated embryos ($n \geq 300$; Fig. 3B, compare with Fig. 2B). Additionally, all the larvae that hatched from LH-treated embryos were similar in size and motility to untreated controls by gross examination (Fig. 3C). Together, these data suggest that LH, like D-limonene alone, is not detrimental to organism development and therefore might provide a better means of drug delivery over EPS-based methods.

As a first measure of potential drug delivery, we assessed viability post-treatment with Nocodazole in LH. After applying and removing Nocodazole, 43% of LH/drug-treated embryos survived to adulthood compared with 72% of LH/DMSO-treated vehicle controls ($n \geq 300$; Fig. 3A). These data suggest that, although LH is benign to development, it might be sufficient to deliver drugs to late-stage embryos.

LH effectively permeabilizes late-stage embryos for drug delivery

We next tested whether LH was facilitating the delivery of Nocodazole by examining microtubules in the abdominal musculature. Following drug treatment, a decrease in microtubule density indicated that Nocodazole was delivered, whereas a dense microtubule network indicated that Nocodazole was not delivered to the muscle cells. To quantify this analysis, we measured the immunofluorescence intensity of α -Tubulin immunostaining relative to Tropomyosin immunostaining in each treatment condition as previously described.¹⁹ Treatment of embryos with 66 nM Nocodazole in LH for 20 min significantly reduced the density of microtubules seen in the muscles in 50–60% of the treated batch of embryos, indicating that LH enables effective delivery of Nocodazole to the muscles ($n \geq 300$; Fig. 3D, E, and H). This is a difference that was not observed with any length of treatment using EPS-based methods ($n \geq 300$; Fig. 2G). Importantly, shorter treatment durations previously shown to be sufficient to permeabilize younger embryos with other solutions were not effective for late-stage embryos, as we found no difference in microtubule density with a 5 min treatment of Nocodazole in LH compared with controls ($n \geq 300$; Fig. 3G and H).¹⁴ Furthermore, 20 min incubation of embryos with LH and Nocodazole was sufficient to achieve maximal disruption of the microtubule network. There was no measurable difference between the microtubule density observed post drug treatment

using either a 20 or 60 min incubation with LH and Nocodazole (data not shown).

Not only is LH-based drug delivery effective, it is also reversible. Following release from Nocodazole inhibition, microtubule density gradually increased over time and the microtubule network was completely restored by 10 min after the removal of Nocodazole ($n \geq 300$; Fig. 3D, E, and H). Specifically, microtubule abundance increased at both 2 and 5 min after removing the embryos from Nocodazole. However, at both time points, there were still significantly fewer microtubules compared with controls. Conversely, at 10 and 30 min after removing Nocodazole, the embryos displayed a microtubule network statistically similar to controls, indicating that the embryos had been released from Nocodazole-mediated inhibition of microtubule polymerization. Collectively, these data show that a 20 min LH treatment followed by a 10 min wash in PBS is an effective means to deliver and remove drugs from batches of late-stage *Drosophila* embryos.

We next assessed whether the effects of Nocodazole and the rescue of microtubule polymerization could be observed with time-lapse imaging approaches. To identify growing microtubules in vivo, fluorescently tagged EB1 was expressed specifically in muscle tissue using the GAL4/UAS system.¹ EB1 is a microtubule plus-end tracking protein that preferentially binds to the growing ends of microtubules and, therefore, identifies sites of microtubule polymerization.²⁰ Thus, embryos carrying the mesodermal/muscle driver, *twist-Gal4*, and *UAS-EB1-eYFP* transgenes were used to address whether microtubule growth could be observed in live embryos.^{21,22}

Embryos expressing both *Twist-Gal4* and EB1-eYFP were treated with 66 nM Nocodazole in LH for 20 min. The LH/drug solution was subsequently removed, and the embryos were prepared for time-lapse imaging. In contrast to fixed analysis, our current time-lapse imaging set-up is not amenable to buffer exchange after initial LH/drug removal, thereby slowing the speed at which the embryos recover from Nocodazole treatment. Thus, longer periods of time elapsed before the release from Nocodazole inhibition could be detected via the emergence of newly formed microtubules in drug-treated embryos. Therefore, differences in microtubule growth were assessed at 30, 50, and 70 min post-treatment by a number of measures, including EB1 comet abundance, run length, and speed.

First, we quantified the number of EB1 comets present in each treatment condition as a proxy for the number of growing microtubules. At both 30 and 50 min after LH/drug removal, there were fewer EB1 comets in Nocodazole-treated embryos compared with DMSO vehicle controls (Fig. 4A–C; Vids. S1 and S2). Of note, the few EB1 comets detected in drug-treated embryos at 30 min post-treatment were detected later in the imaging sequence compared with control movies. Consistent with recovery of microtubule polymerization, at 50 min post Nocodazole treatment, there were more EB1 comets than at 30 min post-treatment with Nocodazole. However, there were still fewer comets than in control embryos. Furthermore, these comets appeared earlier in the imaging sequence and persist throughout the duration of the imaging sequence. Finally, no differences were observed between

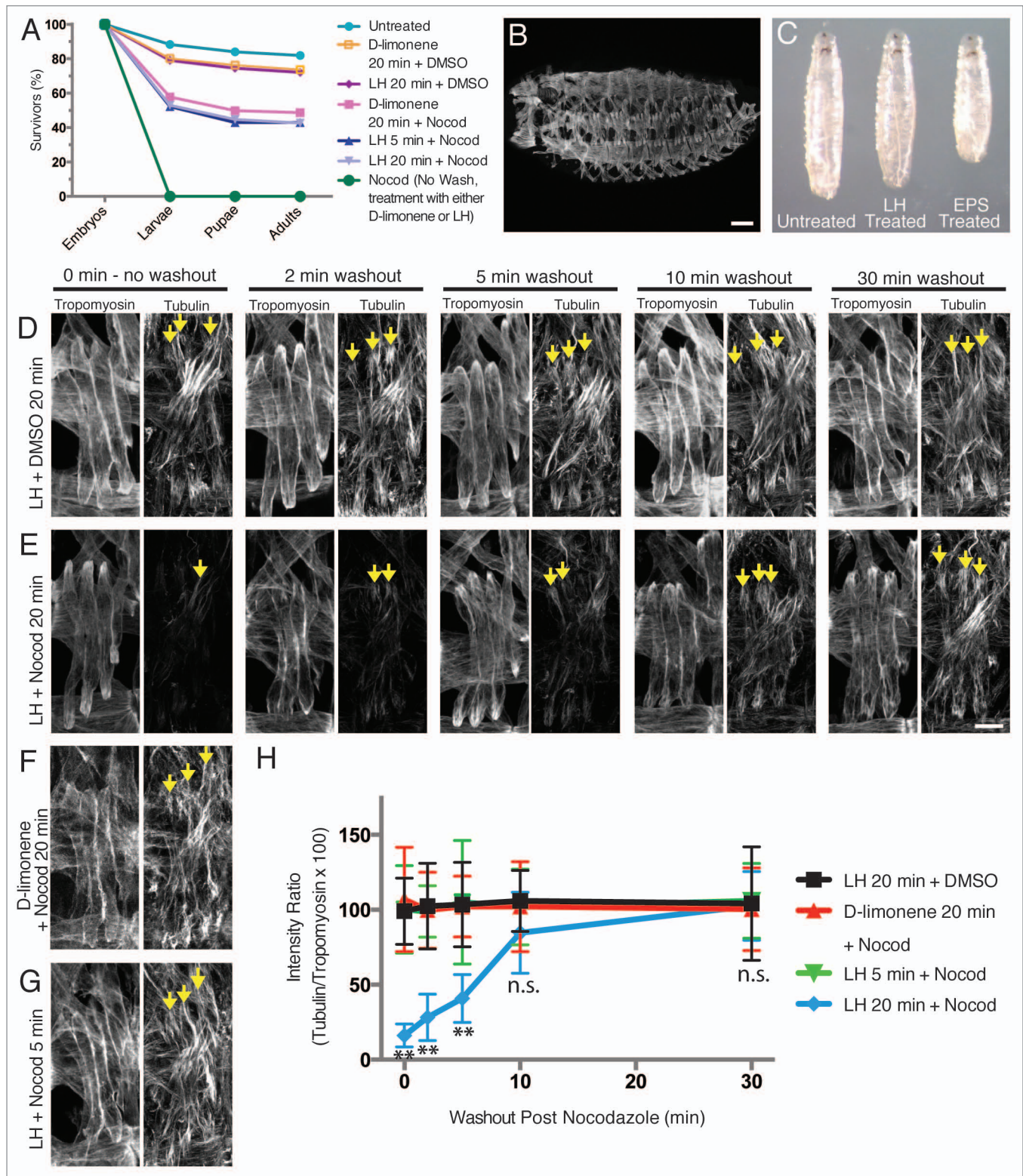


Figure 3. For figure legend, see page 199.

drug-treated and vehicle control embryos at 70 min after treatment, which was indicative of restored microtubule polymerization (Fig. 4A–C) and confirmed that LH-based drug delivery is reversible.

Second, we examined EB1 comet run length as a proxy for microtubule growth persistence (Fig. 4D). The run length of each EB1 comet was decreased relative to controls at both 30 and 50 min post-treatment in drug-treated embryos; however, longer

Figure 3 (see previous page). LH treatment efficiently delivers drugs to the mesoderm and does not adversely affect normal *Drosophila* development. **(A)** Graph of viability of D-limonene- or LH-treated embryos following washout of either drug or vehicle control (unless otherwise noted). **(B)** Stage 16 (16 h AEL) embryo treated with DMSO vehicle control in LH for 20 min immunostained for Tropomyosin (compare with Fig. 2B). Scale bar, 50 μm . **(C)** Comparison of larval size in L3 wandering larvae. **(D–G)** Embryos treated with LH or D-limonene and either DMSO vehicle control or 66 nM Nocodazole in DMSO, washed for the indicated length of time after drug/vehicle removal, fixed, and immunostained with α -Tubulin and Tropomyosin antibodies to label the microtubules and the muscle cells, respectively. Arrows indicate selected microtubules near the dorsal poles of LT muscles. Scale bar, 10 μm . **(D)** Twenty minute treatment with LH and DMSO vehicle control. **(E)** Twenty minute treatment with LH and 66 nM Nocodazole in DMSO. **(F)** Twenty minute treatment with D-limonene and 66 nM Nocodazole in DMSO. **(G)** Five minute treatment with LH and 66 nM Nocodazole in DMSO. **(H)** Quantification of immunofluorescence intensity of α -Tubulin detected in each treatment condition shown in **(D–G)** over time after removal of Nocodazole. n.s., not significant. ** indicates $p < 0.01$ (Note: the LH 20 min + DMSO, D-limonene 20 min + Nocod, and LH 5 min + Nocod data sets largely fall on top of one another).

run lengths were recorded at 50 min compared with 30 min post-treatment with Nocodazole. By 70 min post-treatment, run length was similar to controls (Fig. 4A, B, and D). These data further indicate that treated embryos trend toward recovery following the removal of Nocodazole using our LH-based drug delivery method.

Third, we measured EB1 comet speed as a proxy for microtubule growth rate (Fig. 4E). Unlike the number of comets and comet run length, there was no difference in the speed of traveling EB1 comets at any time point in either treatment condition. These data suggest that the processes governing microtubule growth are not grossly compromised following Nocodazole treatment and washout. Moreover, these data provide further evidence that LH-based drug delivery and removal does not adversely affect embryo health.

Finally, we measured the width of the center portion of the Lateral Transverse (LT) muscles because this region of the muscles appeared to be compromised in Nocodazole-treated embryos (Fig. 4F). In vehicle control embryos, the muscles were robust and uniformly shaped at each time point assessed. Conversely, Nocodazole-treated embryos at 30 min post-treatment resembled a barbell shape, whereby the cell membrane appeared to collapse in the center portion of the LT muscles that is devoid of nuclei. Over time, the width of the center portion of the LT muscles in drug-treated embryos expanded, resembling the more robust nature of vehicle control-treated embryos. The initial collapse in Nocodazole-treated embryos and subsequent expansion seen in those embryos released from Nocodazole inhibition reinforce that an intact microtubule network is required to maintain overall muscle cell shape, as shown to be true for many other cell types.^{23–27} While this is an intriguing aspect of muscle biology to address in future work, this observation taken together with all the data presented herein highlight that LH-based drug delivery is both effective and reversible.

Discussion

Drosophila melanogaster have been used to study the genetics governing growth, development, behavior, and homeostasis for over 100 years, and much of what we know regarding mammalian development was first described in the fly. However, it is difficult to study late embryonic processes by traditional methods, as null or hypomorphic mutations in genes that encode proteins that are fundamental to cell function result in early embryonic lethality. For example, cytoskeletal filaments such as microtubules

provide the framework necessary to support many cellular processes in mature cells, yet these same filaments are also required to support cell division and cell function early in development. Flies carrying null alleles of tubulin are early embryonic lethal and, thus, not useful for studying late-stage embryonic development.²⁸ To assess the contribution of such proteins with early embryonic lethality at later stages of embryonic development, the early requirements for these proteins must be fulfilled prior to inhibiting their functions. An *in vivo* permeabilization technique to deliver drugs to internal tissues to chemically disrupt protein function can overcome this difficulty.

We have developed a method of delivering drugs to internal tissues, specifically the muscles, in batches of late-stage *Drosophila* embryos. Our approach is a modification of that developed by Rand and colleagues, which previously demonstrated a similar permeabilization strategy for early-stage embryos (up to 8 h AEL).¹⁴ For late-stage embryos (13–16 h AEL) however, we have determined that a 1:1 combination of D-limonene and heptane (LH) effectively delivers Nocodazole to the musculature and prevents microtubule polymerization in the muscles in batches of stage 15–16 embryos (13–16 h AEL).

Furthermore, this method of drug delivery is reversible. A number of measures demonstrate that microtubules regrow when embryos are removed from Nocodazole, and reversibility is evident in both fixed and time-lapse imaging. Fixed analysis shows recovery of the microtubule network by 10 min post-treatment with Nocodazole. Similarly, analysis of EB1 comets in live embryos highlights that microtubule polymerization resumes after release from Nocodazole inhibition with our method. Both the number and run length of EB1 comets increase following treatment until they reach control values. Notably, the number of EB1 comets increases more rapidly than run length, which is evident both numerically and pictorially with tracking software. These data agree with reports that microtubule nucleation can occur in the presence of low concentrations of Nocodazole, but complete escape from Nocodazole inhibition is necessary for sustained microtubule growth to be observed.²⁹ Importantly, despite differences in EB1 comet abundance and persistence, the speed of the comets was indistinguishable from controls at any experimental time point. Together, these data suggest that microtubule polymerization is not adversely compromised by our drug delivery method and provide further evidence that the experimental system can be restored to control levels following the application and removal of drugs via our protocol.

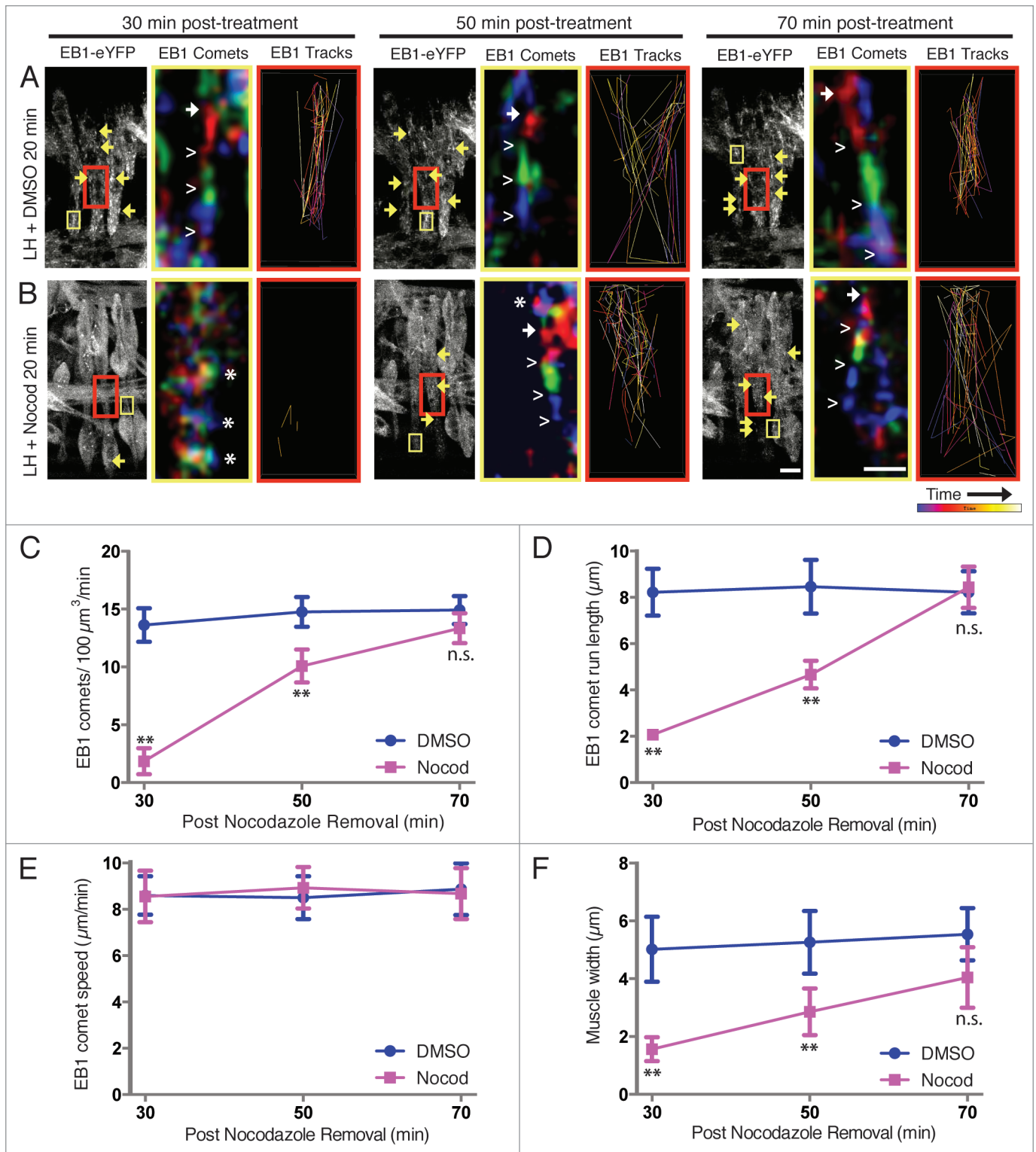


Figure 4. For figure legend, see page 201.

Additionally, this method allows us to further investigate aspects of muscle cell biology. Elimination of the microtubules with drug treatments led to reductions in LT muscle width. This reduction was ameliorated upon removal of Nocodazole and correlated with the return of the microtubule network. These

observations suggest that an intact microtubule network is required to maintain the overall morphology of the muscle cells at this point in development, as seen in many other cell types.²³⁻²⁷ Taken together, our data emphasize the utility of this protocol to study the cellular mechanisms underlying the morphogenesis

Figure 4 (see previous page). Restoration of the microtubule network can be observed in LH-treated embryos using time-lapse imaging. **(A and B,** left panel of each triplet) Still frames from Z-projections of 5 min movies taken of live embryos expressing EB1-eYFP at each of 3 time points: 30, 50, and 70 min post-treatment with LH for 20 min. Arrows highlight selected EB1 comets. Scale bar, 10 μm . Yellow boxes denote the region of muscle used to follow single EB1 comets over time, pseudocolored in the adjacent image. Red boxes indicate the region of the muscle used to monitor multiple EB1 comets traveling over time through a single Z-plane from within the LT muscle only, generating the adjoining image to the right. (Middle panel of each triplet) High magnification image sequences of traveling EB1 comets summed, pseudocolored according to time, and merged into one image. Red highlights the location of EB1-eYFP in frames 1–3 of the movie, green corresponds to frames 4–6, and blue identifies frames 7–9. Solid arrows denote the beginning of a comet, and open carets follow the path of the comet. Asterisks identify regions where all three colors are present in the same location, indicating the absence of EB1 comets. Scale bar, 1 μm . (Right panel of each triplet) Paths of traveling EB1 comets followed over time with Imaris tracking software. Purple tracks were recorded near the beginning of each movie. Yellow-white tracks were recorded toward the end of each movie. **(A)** DMSO vehicle controls in LH with defined EB1 comets. **(B)** LH supplemented with 66 nM Nocodazole in DMSO, showing little evidence of EB1 comets until 50–70 min post-treatment. **(C)** Quantification of the number of EB1 comets detected within the muscles in each treatment condition, indicating the number of growing microtubules. **(D)** Quantification of the run length of EB1 comets in each treatment condition, indicating the persistence of individual growing microtubules. **(E)** Quantification of EB1 comet speed in each treatment condition, indicating the rate of microtubule polymerization. **(F)** Quantification of the width of the center portion of the LT muscles in each treatment condition. For **(C–F)**: n.s., not significant; ** indicates $p < 0.01$.

and maturation of tissues in the late embryo that are difficult to study with traditional *Drosophila* genetics.

Embryo viability post-treatment was also a major consideration. Embryos treated with LH achieve a stereotypic tissue organization as seen in wild-type controls, develop into larvae of comparable size and motility of untreated counterparts, and have similar viability to adulthood compared with untreated controls. These features of LH-based drug delivery methods permit the study of both embryonic tissue formation as well as the physiological impact of embryonic drug treatments at later larval, pupal, or adult stages of development.

In sum, our drug delivery protocol circumvents the challenges that maternal and zygotic nulls present for studies of late-stage embryonic development. This protocol extends recent advances in batch-based permeabilization approaches and stands as a significant improvement over the time-consuming and technically challenging methods of microinjection previously used to deliver drugs to internal tissues. Unlike irreversible microinjection techniques, which require individual manipulation of single embryos, we deliver drugs to numerous embryos simultaneously in a reversible manner. These advances drastically increase sample size as well as provide much-needed temporal control over the experimental system. Furthermore, this technically straightforward approach will facilitate the routine use of drug treatments in the developing *Drosophila* embryo. Future studies will focus on both the use of this protocol in embryos at different stages of development and the effective delivery of other small molecules. Overall, our protocol provides a practical means for chemical disruption of many aspects of late embryonic development thereby permitting the study of cell and developmental processes in vivo.

Materials and Methods

***Drosophila* genetics.** Stocks were grown under standard conditions. Stocks used were *apME-NLS::dsRed*,³⁰ *twist-Gal4*,²¹ and *UAS-EB1-eYFP*.²² *apME-NLS::dsRed* flies were used to evaluate drug treatments using fixed imaging. *Twist-Gal4* flies were crossed to flies carrying *UAS-EB1-eYFP* to detect growing microtubule plus-ends in time-lapse imaging analysis.

Drug treatments

Embryos were collected at 25°C on lightly yeasted apple juice agar plates using timed lays: 1 h pre-lay, followed by a 2 h

lay. Embryos were then aged for an additional 14 h, and subsequently dechorionated in 3% sodium hypochlorite (50% bleach) for 4 min. Dechorionated embryos were washed with copious amounts water to remove excess bleach remnants. Embryos were then transferred to 1.7 mL eppendorf tubes containing 1.3 mL of permeabilization solution with either 2.6 μl dimethyl sulfoxide (DMSO) vehicle only (control) or 2.6 μl of 33 μM Nocodazole (Sigma, M1404, 31430–18–9) diluted in DMSO, bringing the total treatment concentration to 66 nM Nocodazole in a 0.2% DMSO solution. In the present study, 2 different permeabilization solutions were tested: a 1:5 dilution of Embryo Permeabilization Solution (EPS) in PBS (Roche, 11666789001) as described previously,¹⁴ and a 1:1 solution of LH, consisting of equal parts D-limonene (Histoclear®, National Diagnostics, HS-200, 95–100% pure D-limonene) and heptane. Embryos submerged in permeabilization solution with and without drug were placed on a rotating platform and shaken at 250 rpm for the indicated lengths of time at room temperature. Post-treatment, permeabilization solution and drug mixtures were removed from the embryos, and the embryos were rinsed 3 times in PBS (Roche, 11666789001) with vigorous shaking by hand.

Immunohistochemistry and fixed analysis

Treated and rinsed embryos were either fixed immediately without rinsing in PBS (time point 0 min post-treatment), or washed in PBS for defined lengths of time post-treatment (2, 5, 10, or 30 min, as indicated) prior to fixing. In all cases, embryos were fixed with 4% EM-grade paraformaldehyde (Polysciences, 00380) diluted in PBS (Roche, 11666789001) and an equal volume of heptane. In all cases, embryos were devitellinized by vortexing in a 1:1 solution of methanol and heptane. Embryos were mounted in ProLong Gold (Invitrogen) for fluorescent immunostainings. Antibodies with high levels of non-specific background staining (either noted from previous experience in the laboratory setting or by the company's product sheet) were preabsorbed before use: OregonR embryos were incubated with the antibody to absorb any particulates in the antibody solution that may contribute to non-specific binding. These OregonR embryos were then discarded and the antibody solutions used on those embryos were saved, said to be “preabsorbed,” and later used again in experiments, in which less non-specific background staining was often observed. Antibodies were preabsorbed where noted (PA) and used at the following final dilutions: rat

anti-Tropomyosin (PA, 1:500, Abcam, ab50567), and mouse anti- α -Tubulin (1:500, Sigma, T9026). We also used Alexa Fluor 488-, Alexa Fluor 555-, and Alexa Fluor 647-conjugated fluorescent secondary antibodies (1:200) for fluorescent immunostains (all Invitrogen). Fluorescence images were acquired on a Leica SP5 laser-scanning confocal microscope equipped with a 63X 1.4 NA HCX PL Apochromat oil objective and LAS AF 2.2 software. Images were processed using Adobe Photoshop CS4. Maximum intensity projections of confocal z-stacks were rendered using Volocity Visualization 5.4 software (Improvision). To determine the average immunofluorescence intensity, the Measure Average Intensity Function in ImageJ (NIH) was performed on the distal 3 μm at both the dorsal and ventral poles of the Lateral Transverse (LT) myofibers. The intensity of α -Tubulin immunostaining was standardized against the intensity of Tropomyosin immunostaining to control for sample variation. For each treatment condition, all 4 LT muscles were measured in 3 hemisegments from each of 5 embryos. The Student t-test was used to compare each experimental condition to control. Statistical analysis was performed with Prism 6.0.

Time-lapse imaging and analysis

Treated and rinsed embryos were mounted on a gas permeable membrane in halocarbon oil (Halocarbon Oil Products Corp., Series 700, 9002-83-9) and imaged on a Zeiss LSM 700 laser-scanning confocal microscope equipped with 40X 1.4 NA Plan-Apochromat oil DIC M27 objective and ZEN software. EB1 comets were imaged within relatively flat portions of the LT muscles such that z-stacks through the entire depth of the muscle could be acquired at a rate of 5 sec. EB1-eYFP was imaged over 5 min at each of 3 time points: 30, 50, and 70 min post-treatment. For each time point and treatment condition, 20 frames between 0–2 min of the imaging series are displayed in Videos S1 and S2. Trajectory images of traveling EB1 comets were made by summing three consecutive frames and then overlaying those resultant images in a red-green-blue pseudocolored sequence using the Merge Function in ImageJ (NIH). Depictions of traveling EB1 comets (“EB1 Tracks”) were generated using the Dragontail/“Track Spots” Function of Imaris 7.4.2 visualization software using a spot size of 0.5 μm to detect comets, which were then validated manually. For this analysis, a 50 μm^2 rectangular area from a single Z-slice of 0.25 μm step-size only within the LT muscle was examined over time to eliminate interference from EB1 comets traveling through underlying longitudinal muscles. EB1 comet quantifications were assessed by counting the number of EB1 comets

that passed through a 100 μm^3 defined volume per minute. For each time point and treatment, 3 volumes (1 at each of the dorsal and ventral poles of the LT muscle, and one centrally located in the middle of the dorsal-ventral axis of the LT muscle) within all 4 LT muscles in 2 hemisegments in each of 3 embryos were assessed. EB1 comet run length was determined by measuring the distance between the start and end points of a comet’s path using the Line Function in ImageJ software (NIH). At least 10 comets were assessed in each defined volume, and a total of at least 200 comets were analyzed for each time point in each treatment. EB1 comet speed was determined by considering the comet run length over the length of time the comet persisted. Muscle width was determined by using the Line Function in ImageJ (NIH) to measure the distance from 1 edge of the myofiber to the other along the anterior-posterior axis of the middle region of the myofiber along the dorsal-ventral axis. For muscle width, all 4 LT muscles in two hemisegments in each of 3 embryos were measured. The Student t-test was used to compare each experimental condition to control. Statistical analysis was performed with Prism 6.0.

Viability assays

Embryos were collected at 25°C on yeasted apple juice agar plates using timed lays: 1 h pre-lay period, followed by a 2 h lay. Embryos were then aged for an additional 14 h. Stage 15–16 embryos (13–16 h AEL) were selected and dechorionated in 3% sodium hypochlorite (50% bleach) for 4 min. Dechorionated embryos were rinsed with water to remove excess bleach remnants. Embryos were then subjected to drug or vehicle treatment with the permeabilization solution of interest and placed on lightly yeasted apple juice agar plates. A small amount of halocarbon oil (just enough to cover the embryos) was added to prevent desiccation. Embryos were quantified and raised at 22 °C overnight. The following day, L1 larvae were counted and transferred to vials of standard fly food at 22 °C. Eight to twelve days later, the number of pupal cases and adults present in the vials were counted. For each viability assay, at least 100 embryos were analyzed in 3 independent experiments per treatment condition. All values were normalized to 100%.

Disclosure of Potential Conflicts of Interest

No potential conflicts of interest were disclosed.

Supplemental Materials

Supplemental materials may be found here:

<http://www.landesbioscience.com/journals/fly/article/25438>

References

- Brand AH, Perrimon N. Targeted gene expression as a means of altering cell fates and generating dominant phenotypes. *Development* 1993; 118:401-15; PMID:8223268
- Ni JQ, Markstein M, Binari R, Pfeiffer B, Liu LP, Villalta C, et al. Vector and parameters for targeted transgenic RNA interference in *Drosophila melanogaster*. *Nat Methods* 2008; 5:49-51; PMID:18084299; <http://dx.doi.org/10.1038/nmeth1146>
- Dietzl G, Chen D, Schnorrer F, Su KC, Barinova Y, Fellner M, et al. A genome-wide transgenic RNAi library for conditional gene inactivation in *Drosophila*. *Nature* 2007; 448:151-6; PMID:17625558; <http://dx.doi.org/10.1038/nature05954>
- De Brabander M, Geuens G, De Mey J, Joniau M. Nucleated assembly of mitotic microtubules in living PTK2 cells after release from nocodazole treatment. *Cell Motil* 1981; 1:469-83; PMID:7348606; <http://dx.doi.org/10.1002/cm.970010407>
- Ezratty EJ, Partridge MA, Gunderson GG. Microtubule-induced focal adhesion disassembly is mediated by dynamin and focal adhesion kinase. *Nat Cell Biol* 2005; 7:581-90; PMID:15895076; <http://dx.doi.org/10.1038/ncb1262>
- Margaritis LH, Kafatos FC, Petri WH. The eggshell of *Drosophila melanogaster*. I. Fine structure of the layers and regions of the wild-type eggshell. *J Cell Sci* 1980; 43:1-35; PMID:6774986
- Brust-Mascher I, Scholey JM. Microinjection techniques for studying mitosis in the *Drosophila melanogaster* syncytial embryo. *J Vis Exp* 2009; PMID:19755959; <http://dx.doi.org/10.3791/1382>
- Zappe S, Fish M, Scott MP, Solgaard O. Automated MEMS-based *Drosophila* embryo injection system for high-throughput RNAi screens. *Lab Chip* 2006; 6:1012-9; PMID:16874371; <http://dx.doi.org/10.1039/b600238b>

9. Lecuit T, Wieschaus E. Junctions as organizing centers in epithelial cells? A fly perspective. *Traffic* 2002; 3:92-7; PMID:11929599; <http://dx.doi.org/10.1034/j.1600-0854.2002.030202.x>
10. Arking R, Parente A. Effects of RNA inhibitors on the development of *Drosophila* embryos permeabilized by a new technique. *J Exp Zool* 1980; 212:183-94; PMID:6156991; <http://dx.doi.org/10.1002/jez.1402120205>
11. Lynch DV, Lin TT, Myers SP, Leibo SP, Macintyre RJ, Pitt RE, et al. A two-step method for permeabilization of *Drosophila* eggs. *Cryobiology* 1989; 26:445-52; PMID:2507226; [http://dx.doi.org/10.1016/0011-2240\(89\)90069-2](http://dx.doi.org/10.1016/0011-2240(89)90069-2)
12. Mazur P, Cole KW, Mahowald AP. Critical factors affecting the permeabilization of *Drosophila* embryos by alkanes. *Cryobiology* 1992; 29:210-39; PMID:1582229; [http://dx.doi.org/10.1016/0011-2240\(92\)90021-S](http://dx.doi.org/10.1016/0011-2240(92)90021-S)
13. Strecker TR, McGhee S, Shih S, Ham D. Permeabilization, staining and culture of living *Drosophila* embryos. *Biotech Histochem* 1994; 69:25-30; PMID:7511938; <http://dx.doi.org/10.3109/10520299409106257>
14. Rand MD, Kearney AL, Dao J, Clason T. Permeabilization of *Drosophila* embryos for introduction of small molecules. *Insect Biochem Mol Biol* 2010; 40:792-804; PMID:20727969; <http://dx.doi.org/10.1016/j.ibmb.2010.07.007>
15. Petri WH, Wyman AR, Kafatos FC. Specific protein synthesis in cellular differentiation. III. The egg-shell proteins of *Drosophila melanogaster* and their program of synthesis. *Dev Biol* 1976; 49:185-99; PMID:815116; [http://dx.doi.org/10.1016/0012-1606\(76\)90266-9](http://dx.doi.org/10.1016/0012-1606(76)90266-9)
16. Margaritis LH. The egg-shell of *Drosophila melanogaster* III. Covalent crosslinking of the chorion proteins involves endogenous hydrogen peroxide. *Tissue Cell* 1985; 17:553-9; PMID:18620142; [http://dx.doi.org/10.1016/0040-8166\(85\)90031-X](http://dx.doi.org/10.1016/0040-8166(85)90031-X)
17. Cernilogar FM, Fabbri F, Andrenacci D, Taddei C, Gargiulo G. *Drosophila* vitelline membrane cross-linking requires the fs(1)Nasrat, fs(1)polehole and chorion genes activities. *Dev Genes Evol* 2001; 211:573-80; PMID:11819114; <http://dx.doi.org/10.1007/s00427-001-0192-1>
18. Limbourg B, Zalokar M. Permeabilization of *Drosophila* eggs. *Dev Biol* 1973; 35:382-7; PMID:4207363; [http://dx.doi.org/10.1016/0012-1606\(73\)90034-1](http://dx.doi.org/10.1016/0012-1606(73)90034-1)
19. Folker ES, Schulman VK, Baylies MK. Muscle length and myonuclear position are independently regulated by distinct Dynein pathways. *Development* 2012; 139:3827-37; PMID:22951643; <http://dx.doi.org/10.1242/dev.079178>
20. Morrison EE, Wardleworth BN, Askham JM, Markham AF, Meredith DM. EBI1, a protein which interacts with the APC tumour suppressor, is associated with the microtubule cytoskeleton throughout the cell cycle. *Oncogene* 1998; 17:3471-7; PMID:10030671; <http://dx.doi.org/10.1038/sj.onc.1202247>
21. Baylies MK, Bate M. twist: a myogenic switch in *Drosophila*. *Science* 1996; 272:1481-4; PMID:8633240; <http://dx.doi.org/10.1126/science.272.5267.1481>
22. Rogers GC, Rusan NM, Peifer M, Rogers SL. A multicomponent assembly pathway contributes to the formation of acentrosomal microtubule arrays in interphase *Drosophila* cells. *Mol Biol Cell* 2008; 19:3163-78; PMID:18463166; <http://dx.doi.org/10.1091/mbc.E07-10-1069>
23. Tilney LG, Gibbins JR. Microtubules in the formation and development of the primary mesenchyme in *Arbacia punctulata*. II. An experimental analysis of their role in development and maintenance of cell shape. *J Cell Biol* 1969; 41:227-50; PMID:5775787; <http://dx.doi.org/10.1083/jcb.41.1.227>
24. Handel MA, Roth LE. Cell shape and morphology of the neural tube: implications for microtubule function. *Dev Biol* 1971; 25:78-95; PMID:5557970; [http://dx.doi.org/10.1016/0012-1606\(71\)90020-0](http://dx.doi.org/10.1016/0012-1606(71)90020-0)
25. Brown DL, Bouck GB. Microtubule biogenesis and cell shape in *Ochromonas*. II. The role of nucleating sites in shape development. *J Cell Biol* 1973; 56:360-78; PMID:4682901; <http://dx.doi.org/10.1083/jcb.56.2.360>
26. Downie JR. The role of microtubules in chick blastoderm expansion--a quantitative study using colchicine. *J Embryol Exp Morphol* 1975; 34:265-77; PMID:1237532
27. Gipson IK. Cytoplasmic filaments: their role in motility and cell shape. *Invest Ophthalmol Vis Sci* 1977; 16:1081-4; PMID:411764
28. Matthews KA, Kaufman TC. Developmental consequences of mutations in the 84B alpha-tubulin gene of *Drosophila melanogaster*. *Dev Biol* 1987; 119:100-14; PMID:3098600; [http://dx.doi.org/10.1016/0012-1606\(87\)90211-9](http://dx.doi.org/10.1016/0012-1606(87)90211-9)
29. Mikhailov A, Gundersen GG. Relationship between microtubule dynamics and lamellipodium formation revealed by direct imaging of microtubules in cells treated with nocodazole or taxol. *Cell Motil Cytoskeleton* 1998; 41:325-40; PMID:9858157; [http://dx.doi.org/10.1002/\(SICI\)1097-0169\(1998\)41:4<325::AID-CM5>3.0.CO;2-D](http://dx.doi.org/10.1002/(SICI)1097-0169(1998)41:4<325::AID-CM5>3.0.CO;2-D)
30. Richardson BE, Beckett K, Nowak SJ, Baylies MK. SCAR/WAVE and Arp2/3 are crucial for cytoskeletal remodeling at the site of myoblast fusion. *Development* 2007; 134:4357-67; PMID:18003739; <http://dx.doi.org/10.1242/dev.010678>